

# From Classical to Quantum Plasmonics: Classical Emitter and SPASER

V.I. Balykin

*Institute of Spectroscopy, Russian Academy of Sciences, Fizicheskaya Str., 5, Troitsk, Moscow, 108840, Russia.*

Corresponding author: [balykin@isan.troitsk.ru](mailto:balykin@isan.troitsk.ru)

**Abstract.** The key advantage of plasmonics is in pushing our control of light down to the nanoscale. It is possible to envision lithographically fabricated plasmonic devices for future quantum information processing or cryptography at the nanoscale in two dimensions. A first step in this direction is a demonstration of a highly efficient nanoscale light source. Here we demonstrate two types of nanoscale sources of optical fields: 1) the classical metallic nanostructure emitter and 2) the plasmonic nanolaser – SPASER.

## THE CLASSICAL METALLIC NANOSTRUCTURE EMITTER.

Localized surface plasmons are nonpropagating excitations of conduction electrons of metal nanostructures. The subwavelength size of nanostructures gives rise to an efficient restoring force acting on driven electrons, which leads to the occurrence of resonances and field amplification both inside and outside nanostructures. Plasmon resonances have been studied in nanostructures of a variety of shapes and sizes: spherical, elliptical, nanorods, nanoshells, split-ring resonators, U-shaped, and others [1,2].

We propose and experimentally realize a new element for nanoplasmonics - Split Hole Resonator (SHR) [3]. The SHR is the marriage of two basic elements of nanoplasmonics, a nanohole and a nanorod, Fig.1. One of the main merits of the marriage of the two basic elements of nanoplasmonics is that, by varying the SHR parameters (geometrical and material), it is possible to tune the surface plasmon resonance wavelength of the SHR over a much larger wavelength range than for the nanoparticle and nanohole alone, namely, from the UV to the IR range. At resonance, the peak field intensity in SHR occurs at the *single* tip of the nanorod inside the nanohole. The peak field in the SHR is much stronger than the peak fields of the nanorod and nanohole, since the field in the SHR is enhanced by the two mechanisms: the surface plasmon resonance excitation and the lightning-rod effect. For this reason the use of SHR is of special interest in nonlinear nanoplasmonics.

## Third-Harmonic Generation from SHR.

We studied the third-harmonic generation (THG) from SHR [3]. Fig.1 illustrates the main idea of the construction of an SHR and its operation. The SHR consists of a nanohole (Fig. 1b) and a nanorod (Fig. 1a) that are formed in a metal (Al or Au) nanofilm. At the bottom of the Fig.1, calculated distributions of the electric field amplitude in the corresponding nanostructures exposed to irradiation by a plane wave at a wavelength of  $1.5 \mu\text{m}$  are given, namely, the nanorod (Fig. 1a), the nanohole (Fig. 1b), and the SHR nanostructure (Fig. 1c). The wavelength of the incident radiation corresponds to plasmon resonance of the SHR nanostructure.

Figure 2 presents the measurement results for the THG from a single SHR nanostructure in Al nanofilm. The calculated spatial distribution of the electric field amplitude for the nanostructure is shown in Fig. 2b. It can be seen that the electric field amplitude at the fundamental frequency has a clearly pronounced maximum and is localized inside the SHR nanostructure near the tip of its nanorod. In turn, this field acts as a source of a third-order polarization, which results in the THG. It can be seen from the figure that the spatial localization of the third-harmonic radiation source is determined by the size of the nanorod tip, which is about 100 nm. In the optical image of the nanostructure, a diffraction-limited spot is seen, the width at half-height of which is about 230 nm (Fig. 2c). An elliptical shape of this spot indicates that the detected radiation is polarized in the direction orthogonal to the polarization of the excitation radiation. Measurements of the emission spectrum of the SHR nanostructure show that it consists of a narrow line located at the frequency of the third harmonic of the excitation radiation (Fig. 2d).

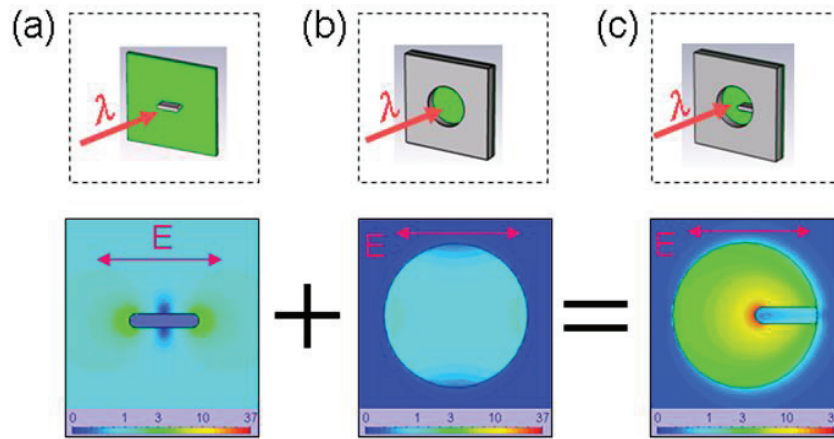


**FIGURE 1.** The main idea of the construction of a SHR and its operation. The SHR (c) is formed from a nanorod (a) and a nanohole (b) in a metal nanofilm. Bottom: spatial distributions of the near field calculated by the FIT method for aluminum nanostructures exposed to irradiation at a wavelength of 1560 nm: (a) a nanorod  $50 \times 180$  nm, (b) a nanohole with a diameter of 400 nm in an aluminum film 50 nm thick, (c) an SHR nanostructure formed by the nanohole (b) and the nanorod (c) [3].

There is a strong resonant behavior of the dependence of the THG on the diameter of the SHR nanohole and on the length of its nanorod. The resonant behavior can be interpreted as follows. A plasmon wave propagates in the nanostructure along the metal/dielectric boundary, which is formed by the nanohole perimeter of the SHR nanostructure. The nanorod plays a role of mirrors which reflect the plasmon wave. If the perimeter length of the hole that forms a nanostructure is equal to an integer number of half-waves of the plasmon wave, then resonances of the Fabry–Perot type are excited in the nanostructure. The length of the SHR nanorod determines the reflection coefficient and the phase shift of the plasmon wave.

The absolute value of the conversion efficiency into the third harmonic per unit area is about  $10^{-5}$ , which is a record value for experiments on the THG from individual nanostructures.

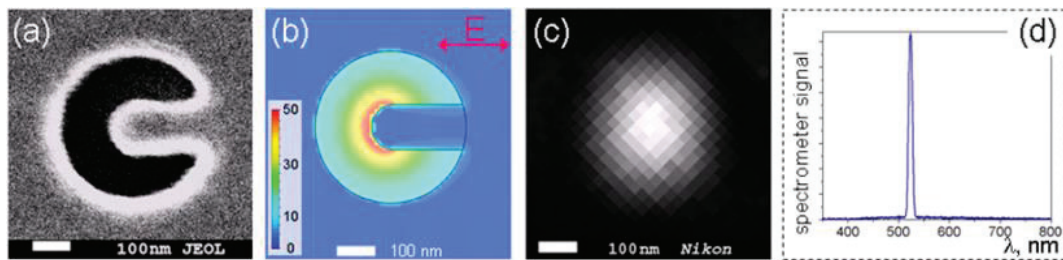


**FIGURE 2.** Generation of the third harmonic by an SHR nanostructure formed in aluminum film. (a) an electron microscope image of the nanostructure, (b) calculated field distribution upon irradiation of the nanostructure by a plane monochromatic wave with a wavelength of 1560 nm, and (c) an optical image of the nanostructure upon its laser irradiation at a wavelength of 1560 nm and detection at the third-harmonic wavelength. The incident radiation is polarized along the direction of the nanorod of the nanostructure [3].

### Polarization Effects in the SHR.

The geometry of the SHR has a clearly pronounced anisotropy, which is determined by the direction of its nanorod. In turn, the presence of anisotropy suggests dependence of the optical response of SHR on the polarization of the incident radiation. We investigated SHR response to the polarization in SHR [4,5]. For the radiation polarized orthogonally to the nanorod, the THG signal is minimal. Upon rotation of the polarization vector by 90 degrees, the radiation power at the frequency of the third harmonic increases 40000 times! This extremely high sensitivity to the polarization of the incident radiation is a consequence of the third order dependence of the THG efficiency on the incident radiation intensity.

A strong polarization dependence of the THG efficiency of the SHR nanostructure shows that SHR can be used for important applications in optical sensing and ultrafast optical switching [4,5]. As an example of such application, we demonstrate the use of SHR nanostructures for the creation of the prototype of an *all-optical display* in which SHR nanostructures play the role of pixels [4]. An optical display that we realized is an array of  $4 \times 4$  identical SHR nanostructures with a spacing between nearest neighbors of 1  $\mu\text{m}$ . The nanostructures were prepared in an aluminum film 50 nm thick. The nanorod of each SHR is turned by an angle of 11.5 degrees with respect to the adjacent one. This optical display operates as follows. All the SHR nanostructures are illuminated by a femtosecond radiation field at a wavelength of 1560 nm. For the linear polarization vector of the incident radiation directed along

the nanorod of one of the SHRs, only this nanostructure of the display proves to be tuned to exact resonance with the field at the frequency of the radiation and precisely this nanostructure becomes an efficient radiation source of the third harmonic. Therefore, choosing a certain direction of the polarization vector of the incident radiation, one can switch on a certain pixel of the display.

### Multiphoton Luminescence.

Multiphoton luminescence is a consequence of the excitation of surface electron states that are localized on the metal surface and that arise on nanosized inhomogeneities of the metal film surface. To excite multiphoton luminescence in an SHR, we formed nanosized inhomogeneities at the tip of its nanorod, where a maximal intensity of the field at the fundamental frequency is reached. The inhomogeneities were created with an ion beam, and their size was in the range 5 – 15 nm.

Figure 3 presents results of our investigations on the generation of multiphoton luminescence by the single SHR nanostructure with surface irregularities. The calculated field distribution of the nanostructure is shown in Fig. 3b. It can be seen from this figure that the spatial distribution of the field at the fundamental frequency exhibits a clearly pronounced maximum near the tip of the SHR nanorod. The optical observation of the SHR with an optical microscope at the luminescence wavelength yields an image of the nanostructure in the shape of a diffraction-limited spot (Fig. 3c). This spot has a circular shape, which indicates that the luminescence radiation is depolarized. The emission spectrum of the SHR nanostructure consists of a narrow peak, which corresponds to the THG, and a broad radiation band, which covers the spectral range from 390 nm to longer than 800 nm (Fig. 3d). Intensity dependence measurements showed that this broadband radiation is a result of three and four photon photoluminescence processes.

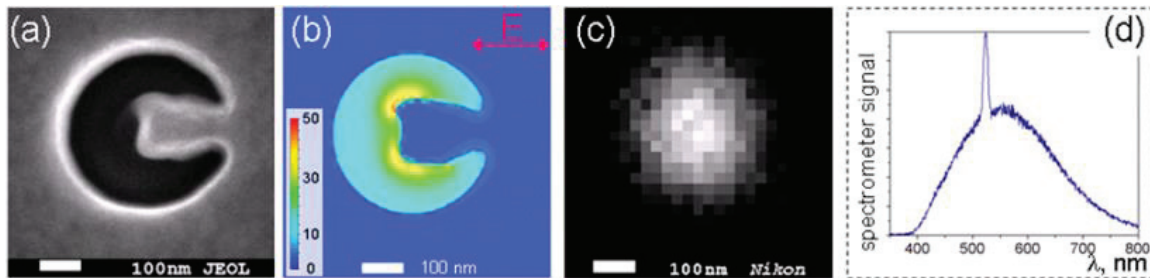


**FIGURE 3.** Multiphoton photoluminescence from a SHR nanostructure formed in an aluminum film. (a) an electron microscope image of the nanostructure, (b) calculated enhancement of the electric field amplitude inside the SHR upon irradiation of the nanostructure by a plane monochromatic wave with a wavelength of 1560 nm, (c) an optical image of the nanostructure upon its laser irradiation at a wavelength of 1560 nm and detection in the spectral range 400–800 nm, and (d) measured emission spectrum of multiphoton luminescence [3].

### Nanocalized UV Light Source.

The nonlinear optical response of a nanostructure can be increased by using high-intensity laser fields. However, intense laser fields cause another problem: because of high optical losses in plasmonic nanostructures, the nanostructures are heated rapidly and, as a consequence, undergo the catastrophic meltdown. In practice, the laser radiation intensity threshold for the nanostructure is about  $10^{10}$  W/cm<sup>2</sup>, strongly limiting efficiency of harmonic generation. Because of strong light absorption by metals, it is believed that plasmonic nanostructures cannot be used for generating intensive radiation harmonics in the ultraviolet (UV) spectral range.

We present results of the nonlinear optical interaction of near IR laser radiation with a gold SHR nanostructure under ultra-short laser pulse (6 fs, two cycles of the laser pulse wave, Fig.4.) to maximally reduce the thermal effects on the nanostructure [6]. The two-cycle laser pulse radiation has a broad emission spectrum that extends from 650 nm to 1  $\mu$ m. The laser light provides maximum intensity at the fundamental frequency without optical breakdown.

The SHR nanostructure is formed in a single crystal gold nanofilm that is flat on the atomic level and the geometry of the nanostructure is ensuring a record-high efficiency of the nonlinear optical interaction. Under the chosen experimental conditions, several multipole plasmon resonances can be simultaneously excited in the SHR nanostructure at fundamental frequencies. We demonstrate a strong nonlinear optical interaction at the frequencies of these resonances that leads to: (i) the second harmonic generation, (ii) the third harmonic generation, and (iii) the light generation at mixed frequencies.

We show that the SHR nanostructure is a source of intense UV radiation in the wavelength range of 250– 300 nm, Fig.4. The THG near field amplitude reaches 0.6% of the fundamental frequency field amplitude, which enables the creation of UV radiation sources with a record high intensity. The UV THG may find many important applications including biomedical ones (such as cancer therapy) [6].

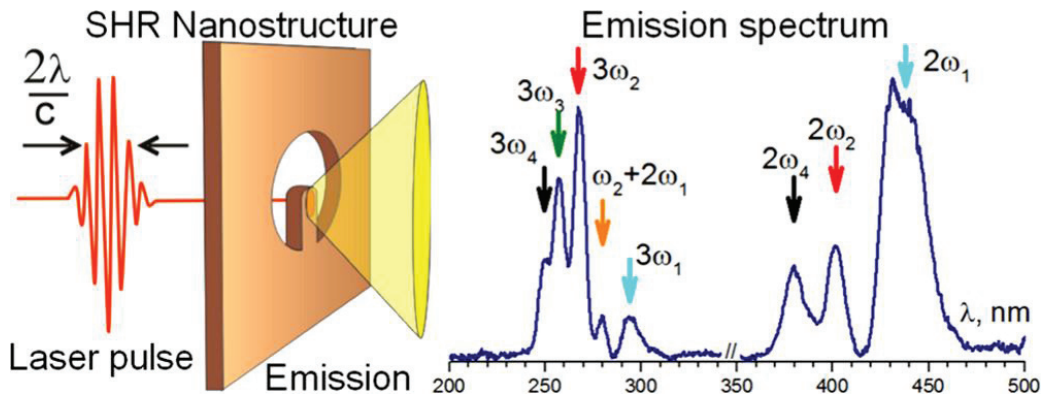


FIGURE 4. Scheme of excitation of the SHR by ultra-short laser pulse and the measured spectra of the second, third harmonics and at mixed frequencies from a single SHR nanostructure [6].

### THE PLASMONIC NANOLASER.

We design [7,8] a planar plasmonic nanolaser, extending the idea and implementation of plasmonic lasers reported in [9]. It is a planar waveguide made of a liquid DMSO layer deposited on a plasmonic crystal, Fig.5. The plasmonic crystal is formed by an array of nanoholes (with 175 nm diameter and a pitch of 565 nm) created in a 100-nm-thick silver film deposited onto a quartz substrate. Dye molecules are optimal for plasmonic lasers because the dye molecules are capable of nearly 100% yield and allow for the creation of an optically homogeneous medium with high gain. We use a liquid gain medium. The main shortcoming of this type of active medium is photobleaching in which a dye molecule is unable to continue fluorescence after approximately  $10^5$ – $10^6$  photon emissions. In the CW regime, a laser using dye in a polymer matrix lives for only 1 ms. The use of a liquid gain medium offers the advantages over a solid gain medium by fixing the bleaching problem. Also, the employment of microfluidics makes plasmonic intracavity spectroscopy suitable for lab-on-chip technology.

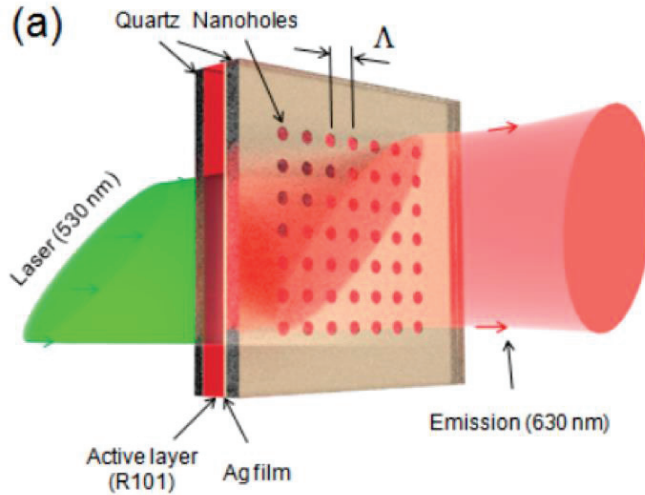
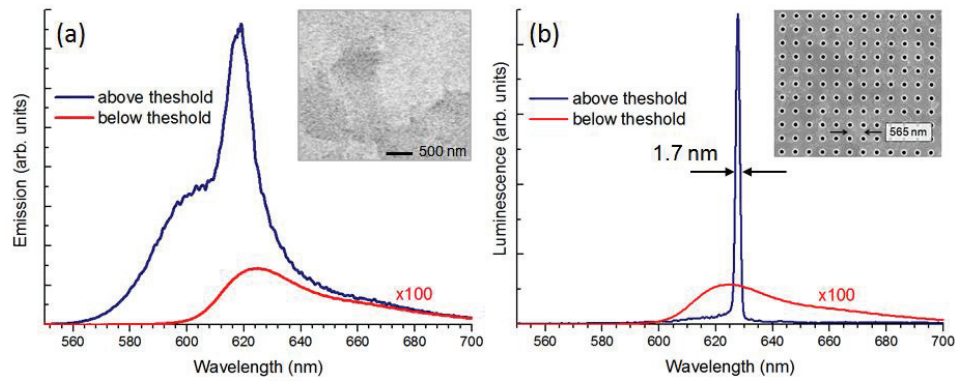


FIGURE 5. Scheme of plasmonic nanolaser: Planar waveguide made of a liquid gain medium layer (a solution of R101 dye in dimethyl sulfoxide (DMSO)) deposited on a plasmonic crystal.

The nanohole array in the silver films is fabricated by using the electron-beam lithography and dry etching. The array of holes is patterned on a 100 nm thick silver film, which is deposited on a UV-grade quartz substrate with a roughness under 1 nm. The silver film is capped by a 10-nm-layer of  $\text{SiO}_2$ . The use of the  $\text{SiO}_2$ -film solves two issues: it suppresses the silver degradation and prevents the quenching of excited dye molecules. The quenching leads to an undesirable heating of the silver film that, in turn, leads to sample destruction at pumping intensities above  $2 \text{ MW/cm}^2$ .

The gain medium (R101 dye in DMSO with the concentration  $6 \times 10^{18} \text{ cm}^{-3}$ ) provides a material gain  $75 \text{ cm}^{-1}$  via pulsed optical pumping at the wavelength of 530 nm. To decrease the threshold intensity, we have chosen a specific geometry of the pumping beam, which selectively excites the selected mode. This geometry leads to a decrease in the threshold pumping by the factor of 80, and consequently, to an increase in the lifetime of the gain medium. The volume of the gain medium in the pumped region is by four orders of magnitude smaller than the volume of the total gain medium. This leads to a long-lived stable generation regime that can be sustained for several weeks.



**FIGURE 6.** (a) The spectrum of dye luminescence in the quartz/silver/DMSO/quartz system without nanoholes; (b) the luminescence spectrum of the plasmonic laser. The insets show electronic microscope images of the samples [7].

The lasing occurs at pumping intensities above 500 kW/cm. The spectrums of the plasmonic laser for two values of pumping are shown in Fig 6. At intensities below 500 kW/cm<sup>2</sup>, the spectral contour is very similar to that of usual R101 dye luminescence. However, at higher pumping intensities, the luminescence contour changes dramatically, and a very narrow spectral line with the half-width of 1.7 nm emerges at 628 nm. Such a narrow line width indicates that we deal with lasing.

## REFERENCES

1. P. Zijlstra and M. Orrit, *Rep. Prog. Phys.* **74**, 106401-106456 (2011).
2. V.I. Balykin, P.N. Melentiev, *Phys. Usp.* (accepted 2017).
3. P.N. Melentiev, A.E. Afanasiev, A.A. Kuzin, A.S. Baturin and V.I. Balykin, *Optics Express*, **21**, 13896 -13905 (2013).
4. P.N. Melentiev, A.E. Afanasiev, A.A. Kuzin, A.S. Baturin and V.I. Balykin, *Optics Letters*, **38**, 2274-2276 (2013).
5. P.N. Melentiev, A.E. Afanasiev, A.V. Tausenev, A.V. Konyaschenko, V.V. Klimov and V.I. Balykin, *Laser Phys. Lett.* **11**, 105301-105309 (2014).
6. N.P. Melentiev, A.E. Afanasiev, A.A. Kuzin, V.M. Gusev, O.N. Kompanets, R.O. Esenaliev, and V.I. Balykin, *Nano Lett.*, **16**, 1138-1142 (2016).
7. P. Melentyev, A. Kalmykov, A. Gritchenko, A. Afanasyev, V. Balykin, A. Baburin, E. Ryzhova, I. Filippov, I. Rodionov, I. Nechepurenko, A. Dorofeenko, I. Ryzhikov, A. Vinogradov, A. Zyablovsky, E. Andrianov, and A.A. Lisyansky, *Appl.Phys.Letters*, (to be published 2017).
8. Balykin V.I., *Phys. Usp.* (to be published 2017).
9. X. Meng, J. Liu, A. V. Kildishev and V. M. Shalaev, *Laser & Phot. Rev.* **8**, 896-904 (2014).